# Large $N$ Fractons

Kristan Jensen[1,*] and Amir Raz[2,†]
[1]Department of Physics and Astronomy, University of Victoria, Victoria, British Columbia V8W 3P6, Canada
[2]University of Texas, Austin, Physics Department, Austin, Texas 78712, USA

(Received 29 September 2022; revised 7 December 2023; accepted 8 January 2024; published 15 February 2024)

We consider theories of $N$-component fields with exotic spacetime symmetries, including a conserved dipole moment. Microscopic charges are immobile by symmetry, and so resemble fractons. Using collective fields we solve these models to leading order in large $N$. The large $N$ solution reveals that these models are strongly correlated, and that interactions dress the microscopic charges so that they become mobile, long-lived quasiparticles. Dipole symmetry is spontaneously broken throughout the phase diagram of these models, leading to a low-energy Goldstone description.

DOI: 10.1103/PhysRevLett.132.071603

*Introduction.*—Consider quantum mechanical models of fracton order (see, e.g., [1–6]). These models describe new, at this time purely hypothetical phases of quantum matter. Perhaps the two most visceral signatures of these phases are finite-energy quasiparticles of restricted mobility, colloquially called "fractons," and in some cases, a large ground state degeneracy sensitive to the details of an underlying lattice. While these phases have yet to be realized in experiment (Although perhaps they have [7].) there is reason to believe that they will be found. Besides the prospect of engineering such a phase with ultracold atoms [8] or antiferromagnets [9], there are proposals that defects in elastic media in $2+1$ dimensions [10,11], vortices in superfluid helium [12,13], and the lowest Landau level of fractional quantum Hall states [14] all have fractonlike physics.

Fractons pose a number of challenges to condensed matter and high energy theorists. From a purely theoretical point of view, one ought to be able to obtain a continuum field theory description of fracton phases upon coarse-graining, but then the features mentioned above seem to defy the standard Wilsonian effective field theory paradigm. Informally, this challenge can be phrased as a question: how can field theory describe restricted-mobility excitations or a UV-sensitive spectrum of low-energy states? (See [15,16].) There is another practical problem for theorists to solve. Apart from completely integrable Hamiltonians like the X-Cube model [17] or extreme limits of condensed phases, generic models of fractons are strongly correlated, and as such we have few tools to study them and little knowledge of their macroscopic features, which if they were known could be used to find them in nature. Can we find soluble models of interacting fractons, and thereby study their physics?

The goal of this Letter is to address these theoretical and practical challenges. An important clue is that, in understood examples, the existence of restricted-mobility excitations and a lattice-sensitive ground state degeneracy are ultimately consequences of exotic spacetime symmetries. In the experimental proposals for fractons above, like vortices in superfluid helium, the symmetry generators include both a $U(1)$ charge and, crucially, the corresponding dipole moment. (This example also includes a conserved quadrupole trace.) Isolated charges are then immobile by symmetry; these are the sought-after fractons. Charges can bind into completely mobile dipoles. Meanwhile, if a ground state is not invariant under the dipole symmetry, there is a ground state manifold generated by action of the dipole symmetry, with a ground state degeneracy parametrically equal to the volume of the dipole symmetry group. This volume is infinite in the continuum, but it is compact in a lattice regularization.

This clue is important because it suggests a way forward, which we take in this Letter. Namely, we find and solve simple theories with these exotic spacetime symmetries, paying careful attention to subtleties that arise in the functional integral.

Inspired by models of Pretko [18], we study interacting continuum field theories with $N$ charged scalar fields, imposing a $U(N)$ symmetry that rotates the fields, and a conserved dipole moment associated with the diagonal $U(1) \subset U(N)$ charge. The Lagrangians of these theories are nonstandard. Instead of the usual quadratic terms with two spatial derivatives, the simplest terms with spatial derivatives include at last four powers of the fundamental fields and these may lead to strong interactions. However, these theories are generalized vector models, which we proceed to solve in the large $N$ limit using methods familiar from the large $N$ Chern-Simons matter and SYK literature (e.g., [19,20]).

We establish many results for these theories, including their phase diagram at finite temperature and chemical potential. Crucially the dipole symmetry is spontaneously broken everywhere in the phase diagram, and we find a new high temperature phase in which the dipole symmetry is spontaneously broken, but the $U(1)$ symmetry is not. The interactions mentioned above with spatial derivatives generate a momentum-dependent self-energy, which tames loop integrals and allows quasiparticles to propagate. When there is an underlying lattice the large $N$ solution has a continuum limit, but the spectrum of fluctuations retains some sensitivity to the details of the lattice. For example, the zero modes associated with the symmetry breaking have a UV-sensitive volume, the number of lattice sites in a lattice regularization, which allows the near-continuum theory to describe a UV-sensitive spectrum of low-energy states.

The remainder of this Letter is organized as follows. We write down the large $N$ models of interest in the next section, and rewrite them in terms of collective fields that are weakly coupled at large $N$. We then find the solution to the collective field description and the ensuing phase diagram, and conclude with a discussion. Many further results are relegated to the Supplemental Material [21] which includes Refs. [22–32].

*Models with conserved dipole moment.*—We work at finite temperature through the imaginary time formalism. We consider models with $N$ complex scalars $\phi^a$ (with $a = 1, 2, \ldots, N$) enjoying a number of symmetries. To wit, we impose invariance under spacetime translation symmetry, spatial rotations, parity, and $U(N)$ symmetry. Crucially, we also demand that the dipole moment associated with the diagonal $U(1) \subset U(N)$ is conserved. The latter amounts to an invariance under $\phi^a(t, \vec{x}) \to e^{i\vec{d}\cdot\vec{x}}\phi^a(\tau, \vec{x})$, which we term a dipole transformation. Pretko [18] has found a useful way to write down effective actions invariant under dipole transformations. While spatial derivatives of $\phi^a$ are not covariant under dipole transformations, the basic covariant object with spatial derivatives is

$$D_{ij}(\phi^a, \phi^b) = \frac{1}{2}\left(\phi^a \partial_i \partial_j \phi^b - \partial_i \phi^a \partial_j \phi^b + (a \leftrightarrow b)\right), \quad (1)$$

which transforms as $D_{ij}(\phi^a, \phi^b) \to e^{2i\vec{d}\cdot\vec{x}} D_{ij}(\phi^a, \phi^b)$.

In this work we study simple field theories with a single time derivative, at most quartic interactions, and at most four spatial derivatives. There is a model with only two spatial derivatives, which we call model 1, given by

$$S = \int d\tau d^d x \left( \bar{\phi}^a \partial_\tau \phi^a + 2\mathrm{Re}\left[\frac{\lambda}{N}\delta^{ij} D_{ij}(\bar{\phi}^a, \bar{\phi}^b)\phi^a \phi^b\right] + V \right), \quad (2)$$

where $V = -\mu\bar{\phi}^a\phi^a + (\lambda_4/N)(\bar{\phi}^a\phi^a)^2$, and sums over $a$, $b$ are implied. The model is specified by a chemical potential $\mu$, an inverse temperature $\beta$ (introduced by analytic continuation to imaginary time), a quartic interaction $\lambda_4$, and a complex coupling $\lambda$. We have introduced factors of $1/N$ so that there is a nice large $N$ limit.

We also introduce model 2, which has four spatial derivatives, described by

$$S = \int d\tau d^d x \left( \bar{\phi}^a \partial_\tau \phi^a + \frac{\lambda_T}{N} D_{\{ij\}}(\phi^a, \phi^b) D^{\{ij\}}(\bar{\phi}^a, \bar{\phi}^b) + \frac{\lambda_S}{N}|\delta^{ij} D_{ij}(\phi^a, \phi^b) + \gamma \phi^a \phi^b|^2 + V \right), \quad (3)$$

where $D_{\{ij\}}(\phi^a, \phi^b) = D_{ij}(\phi^a, \phi^b) - (\delta_{ij}/d)\delta^{kl} D_{kl}(\phi^a, \phi^b)$ is the traceless part of $D_{ij}(\phi^a, \phi^b)$. In addition to the chemical potential and temperature, this model is characterized by real couplings $\lambda_T$ ($T$ is for tensor) and $\lambda_S$ ($S$ is for scalar), and a complex parameter $\gamma$. Note that one can reach model 1 by a scaling limit of model 2, by taking $\lambda_T, \lambda_S \to 0$ while holding $\lambda_S \gamma = \lambda$ fixed.

Both model 1 and model 2 are effectively vector models, and so are soluble at large $N$. To solve them, we integrate in bilocal collective degrees of freedom $G(x_1, x_2)$ and $\Sigma(x_1, x_2)$, whose expectation values are the large $N$ propagator of $\phi^a$ and self-energy, respectively. These fields decouple the quartic interactions, allowing us to integrate out the $\phi^a$. We then integrate all but one of the scalars, $\phi^1 = \sigma$, which will allow us to diagnose the spontaneous breaking of $U(N) \to U(N-1)$. The fields $(G, \Sigma; \sigma)$ are weakly coupled at large $N$, and solving the large $N$ model amounts to solving their classical equations of motion. Making a translationally invariant ansatz, with $\sigma(x) = \sigma$ and

$$G(k_1, k_2) = N G(k_2)\Delta, \qquad \Sigma(k_1, k_2) = \Sigma(k_2)\Delta, \quad (4)$$

where we have Fourier transformed and $\Delta = \beta\delta_{n_1 n_2} \times (2\pi)^d \delta(\vec{k}_1 + \vec{k}_2)$ with $\omega_n = (2\pi n/\beta)$ the frequency of the $n$th Matsubara mode, these equations (the large $N$ Dyson equations for the propagator and self-energy) read

$$G(k) = \frac{1}{i\omega_n + \Sigma(k)} + \frac{|\sigma|^2}{N}\beta\delta_{n0}(2\pi)^d \delta^d(\vec{k}),$$
$$\Sigma(k) = -\mu + 2\int Dk' \, G(k') N V_4(-k, -k', k, k'), \quad (5)$$

along with $\sigma\Sigma(k=0) = 0$. Here $Dk = (1/\beta)\sum_n [d^d k/(2\pi)^d]$ and $NV_4$ is the quartic vertex in momentum space. Model 1 has $NV_4 = \frac{1}{2}(\lambda|\vec{k}_{12}|^2 + \bar{\lambda}|\vec{k}_{34}|^2) + \lambda_4$ with $\vec{k}_{mn} = \vec{k}_m - \vec{k}_n$, which gives a local version of an $M$-particle Hamiltonian considered in [33]. In model 2 the quartic vertex is

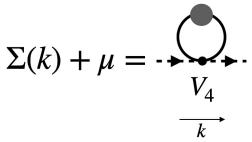


FIG. 1. The Dyson equations in diagrammatic form. The internal line is the exact large $N$ propagator $G$.

$$NV_4(k_i) = \frac{\lambda_T}{4}\left((\vec{k}_{12}\cdot\vec{k}_{34})^2 - |\vec{k}_{12}|^2|\vec{k}_{34}|^2\right) + \frac{\lambda_S}{4}\left(|\vec{k}_{12}|^2 + 2\bar{\gamma}\right)\left(|\vec{k}_{34}|^2 + 2\gamma\right) + \lambda_4. \quad (6)$$

Diagrammatically, the Dyson equations resum bubbles as shown in Fig. 1. A more detailed algebraic derivation is given in the Supplemental Material [21].

These models are many-body quantum mechanics in $d$ dimensions, where a conserved number of particles $M$ (conjugate to $\mu$) interact via $2 \to 2$ interactions characterized by $V_4(k_i)$, where $(k_1, k_2)$ label the incoming momenta and $(k_3, k_4)$ the outgoing momenta. The part of the potential that appears in the Dyson equation (5), $V_4(-k, -k', k, k')$, is the forward limit of $V_4$. In model 1 it is $\mathrm{Re}(\lambda)|\vec{k} - \vec{k}'|^2 + \lambda_4$, and in model 2 it is $(\lambda_S/4)\left||\vec{k} - \vec{k}'|^2 + 2\gamma\right|^2 + \lambda_4$. We anticipate our models to be consistent only when the forward limit is positive. For model 1 this implies $\mathrm{Re}(\lambda), \lambda_4 \geq 0$, with more complicated constraints for model 2.

Let us return to the dipole symmetry. It acts on the momentum space field by $\tilde{\phi}^a(\omega, \vec{k}) \to \tilde{\phi}^a(\omega, \vec{k} + \vec{d})$, i.e., by a shift of momentum, and on the conjugate field by the opposite shift. In a lattice regularization $\vec{d}$ is then valued in the space of momenta, the Brillouin zone. Dipole transformations then act on $G(k)$ and $\Sigma(k)$ by $G(\omega, \vec{k}) \to G(\omega, \vec{k} + \vec{d})$, and similarly for $\Sigma$. It follows that the Green's function is an order parameter for dipole breaking: if $G(\omega, \vec{k})$ depends on the spatial momentum, i.e., if the position space Green's function $\langle\bar{\phi}^a(x)\phi^b(0)\rangle$ is not ultralocal in space, then the dipole symmetry acts on it. This makes physical sense: $G$ is the one-point function of an operator that creates a dipole, with a charge at 0 and an anticharge at $x$, which if nonzero is a dipole condensate in analogy with the usual charge condensate associated with ordinary symmetry breaking.

Insofar as it takes fine-tuning to make the Green's function ultralocal, we expect the dipole symmetry to be broken throughout the phase diagram. There is also the possibility of $U(N) \to U(N-1)$ symmetry breaking, parametrized by the condensate $\sigma = \langle\phi^{a=1}\rangle$, and in such a phase dipole symmetry is necessarily broken as well. That is, on general grounds we expect to find two phases of our models: (i) a "normal" phase where dipole symmetry is broken but $U(N)$ is preserved, and (ii) a "condensed" phase in which $U(N)$ is broken to $U(N-1)$ and the dipole symmetry is also broken. In both phases the dipole symmetry is broken, and so both phases are a superfluid of condensed dipoles. The normal phase has a vector order parameter, $\partial_i G$ in the coincident limit, so we call it a *p-wave dipole superfluid*, while the condensed phase has a scalar order parameter $\langle\phi^a\rangle$, so we call it a *s-wave dipole superfluid*.

In the absence of a condensate $\sigma$ the large $N$ equations (5) are invariant under dipole shifts on account of the fact they only depend on the difference of momenta $\vec{k} - \vec{k}'$. As such, a solution $G(\omega, \vec{k})$ implies the existence of a family of solutions $G(\omega, \vec{k} + \vec{d})$. With a condensate, we get a family of solutions provided that we also shift the condensate as $\delta^d(\vec{k}) \to \delta^d(\vec{k} + \vec{d})$.

*Large N solutions.*—We now endeavor to solve the Dyson equations (5). Because the vertex $V_4$ does not depend on the frequency $\omega_n$, it follows that the self-energy $\Sigma$ only depends on spatial momentum. This allows us to perform the sum over Matsubara modes in (5), so that

$$\Sigma(\vec{k}) = \int \frac{d^dk'}{(2\pi)^d} NV_4(-k, -k', k, k') \coth\left(\frac{\beta\Sigma(\vec{k}')}{2}\right) - \mu + 2\frac{|\sigma|^2}{N} NV_4(-k, 0, k, 0), \quad (7)$$

along with $\sigma\Sigma(k = 0) = 0$.

The vertex $V_4(-k, -k', k, k')$ is a polynomial in $k$ of degree 2 in model 1, and degree 4 in model 2, and so $\Sigma(\vec{k})$ is too. We then make a rotationally invariant ansatz $\Sigma(\vec{k}) = a_0 + a_1|\vec{k}|^2 + a_2|\vec{k}|^4$ (with $a_2 = 0$ for model 1). The Dyson equation (7) becomes a finite system of coupled equations for the unknown quantities $a_0$, $a_1$, $a_2$, and $\sigma$. The condition $\sigma\Sigma(k = 0) = \sigma a_0 = 0$ leads to two classes of solutions, a normal phase with $\sigma = 0$ and $a_0 \neq 0$, and a condensed phase with $\sigma \neq 0$.

Plugging our ansatz back into (7) and suitably regularizing, the momentum integral can be evaluated analytically in model 1 and numerically in model 2. Here we focus on model 1, leaving model 2 to the Supplemental Material [21]. In the normal phase where $\sigma = 0$, (7) becomes

$$a_0 = -\mu + \frac{d}{2\beta}\frac{\mathrm{Li}_{\frac{d+2}{2}}(e^{-\beta a_0})}{\mathrm{Li}_{\frac{d}{2}}(e^{-\beta a_0})} + \frac{\lambda_4}{\mathrm{Re}(\lambda)}a_1,$$
$$a_1 = \frac{2\mathrm{Re}(\lambda)}{(4\pi\beta a_1)^{\frac{d}{2}}}\mathrm{Li}_{\frac{d}{2}}(e^{-\beta a_0}), \quad (8)$$

while in the condensed phase where $a_0 = 0$ we have

$$\mu = \frac{\lambda_4}{\mathrm{Re}(\lambda)}a_1 + \frac{d\mathrm{Re}(\lambda)}{(4\pi\beta a_1)^{\frac{d}{2}}}\frac{1}{\beta a_1}\zeta\left(\frac{d+2}{2}\right),$$
$$\frac{|\sigma|^2}{N} = \frac{a_1}{2\mathrm{Re}(\lambda)} - \frac{1}{(4\pi\beta a_1)^{\frac{d}{2}}}\zeta\left(\frac{d}{2}\right). \quad (9)$$

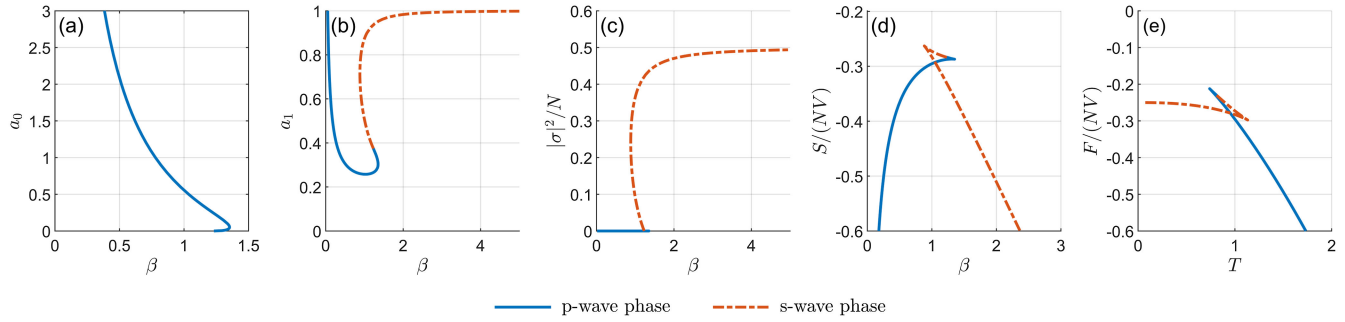


FIG. 2. The solutions to the Dyson equations for model 1 are presented in panels (a) and (b), along with the condensate in (c), the on-shell action in (d), and free energy densities in (e) as a function of inverse temperature $\beta$ in $d = 3$, with $\mu = 1$ and $\mathrm{Re}(\lambda) = \lambda_4 = 1$.

In both models we solve the Dyson equations numerically using standard solvers of systems of nonlinear equations (e.g., the function fsolve in MATLAB or NSolve in *Mathematica*.) We present some numerical solutions for model 1 in Fig. 2 and for model 2 in the Supplemental Material [21].

We can also solve the Dyson equations analytically in various limits of temperature and chemical potential. For example, in model 1 at low temperature we find $a_1 \approx \mathrm{Re}(\lambda)\mu/\lambda_4$, $|\sigma|^2/N \approx \mu/(2\lambda_4)$ when $\mu > 0$ and $d > 2$; $a_1 \approx \mathrm{Re}(\lambda)\mu/\lambda_4$, $a_0 \approx 0$, and $\sigma = 0$ when $\mu > 0$ and $d = 2$; and $a_0 \approx -\mu$, $a_1^{[(d+2)/2]} \approx [2\mathrm{Re}(\lambda)/(4\pi\beta)^{(d/2)}]e^{\beta\mu}$, and $\sigma = 0$ when $\mu < 0$. We present more asymptotic solutions in the Supplemental Material [21]. In fact, at zero temperature we find that the large $N$ solution is one-loop exact in $\lambda$, $\lambda_S$, and $\gamma$ to leading order in large $N$, although in general the solution is a nonanalytic function of couplings.

*Phase diagrams.*—Our models have, in general, a nontrivial phase diagram. To determine it we evaluate the thermal free energy density from our large $N$ solutions. We have in finite but large volume

$$\beta F = -\ln Z = NS^{(0)} + S^{(1)} + \frac{S^{(2)}}{N} + O(N^{-2}), \qquad (10)$$

where the $1/N$ expansion is the weak coupling expansion of the collective field theory of $(G, \Sigma; \sigma)$. Here $NS^{(0)}$ is the on-shell action of the large $N$ solution, while $S^{(1)} = -\ln Z_{1-\mathrm{loop}} = -\ln V_{1-\mathrm{loop}} - \ln \tilde{Z}_{1-\mathrm{loop}}$ is the one-loop correction which we separate into a zero mode volume $V_{1-\mathrm{loop}} = VV_{\mathrm{BZ}} = N_{\mathrm{sites}}$ the dimensionless volume of the Brillouin zone, i.e., the number of lattice sites, and a contribution $-\ln \tilde{Z}_{1-\mathrm{loop}}$ from nonzero modes, $S^{(2)}$ the two-loop correction, and so on. The dipole breaking implies a UV-sensitive normalization $Z \propto N_{\mathrm{sites}}$. In the Supplemental Material [21] we show that this prefactor can be simply understood from the symmetry algebra. Irreducible representations of the dipole symmetry with nonzero charge have a dimension $N_{\mathrm{sites}}$, implying that the density of states has that prefactor, and so also $Z$.

In most regions of the phase diagram we only find a single solution. In those where both phases exist, the dominant one is that with the lower large $N$ free energy, i.e., smaller on-shell action.

In model 1 we find both phases in $d > 2$ with a first-order transition between a high-temperature $p$-wave dipole superfluid and a low-temperature $s$-wave phase. In $d = 2$ we only find the $p$-wave phase. See Fig. 2 for the thermal free energy at fixed chemical potential, and the phase diagram in Fig. 3, both in $d = 3$.

Though the same two phases exist in model 2, the phase diagram for this model is more elaborate due to the additional parameters. When $\mathrm{Re}(\gamma) > 0$ the phase structure is similar to model 1, with a first order transition from a high temperature $p$-wave phase to the $s$-wave phase at low temperature in $d > 2$, and only the $p$-wave phase in $d = 2$. However when $\mathrm{Re}(\gamma) < 0$ the low temperature phase is $p$ wave with $a_1 < 0$. This results in two possibilities, depending on the value of the chemical potential [assuming $\mathrm{Re}(\gamma)$

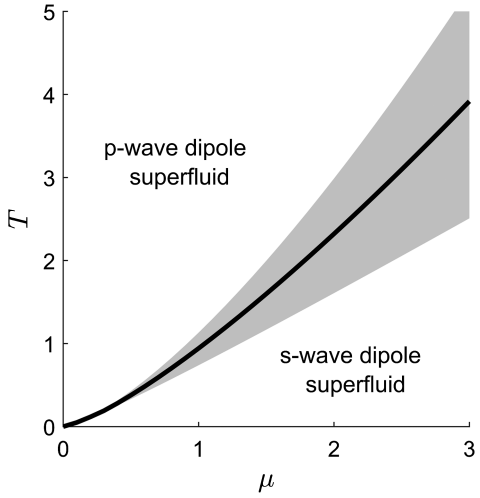


FIG. 3. The phase diagram of model 1 in $d = 3$ as a function of inverse temperature $\beta$ and chemical potential $\mu$ measured in natural units where $\mathrm{Re}(\lambda) = \lambda_4 = 1$. The black line indicates a first order phase transition, and the shaded gray area is the region where both phases coexist.

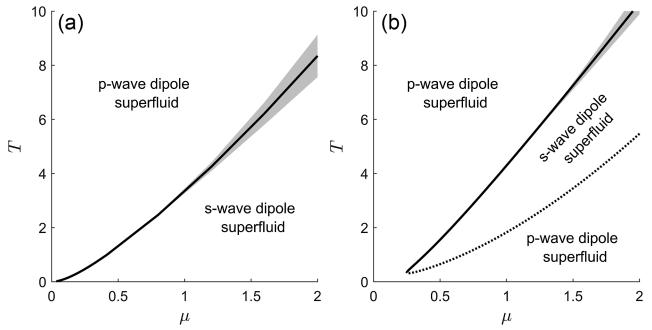


FIG. 4. Sample phase diagrams of model 2 in $d = 3$ as a function of inverse temperature $\beta$ and chemical potential $\mu$ measured in natural units where $\lambda_S = 1$ and $\lambda_S|\gamma|^2 + \lambda_4 = 1$. In (a) $\mathrm{Re}(\gamma) = 0.25$, while in (b) $\mathrm{Re}(\gamma) = -0.25$. The black line indicates a first order phase transition, the shaded gray area the region where both phases coexist, and the dotted black line a continuous phase transition.

is fixed.] If the chemical potential $\mu$ is small enough then there is no $s$-wave phase at all, and the system stays in the dipole superfluid phase at all temperatures. However, if the chemical potential $\mu$ is increased beyond some critical threshold then there is an intermediate temperature range where the system is in the $s$-wave phase. Starting at high temperatures, the transition to this phase is first order, but the transition back to the dipole superfluid phase at low temperatures is continuous. Two sample phase diagrams for model 2 are presented in Fig. 4, one for $\mathrm{Re}(\gamma) > 0$ and another for $\mathrm{Re}(\gamma) < 0$.

*Discussion.*—In this Letter we have solved continuum models whose microscopic degrees of freedom are immobile charges with $N \gg 1$ degrees of freedom and a $U(N)$ global symmetry. These models have an exotic spacetime symmetry with a conserved dipole moment. We find two phases, a high-temperature phase in which dipole symmetry is spontaneously broken but the $U(N)$ is preserved, and a low-temperature phase in which $U(N) \to U(N-1)$ and dipole symmetry is also broken. The high-temperature phase has a vector order parameter, the gradient of the single-particle Green's function in the coincident limit, and the low-temperature phase has a scalar order parameter. So we dubbed the high-temperature phase a *p-wave* dipole superfluid, and the low-temperature phase a *s-wave* dipole superfluid.

We study many more features of these models in the Supplemental Material [21], including the low-energy effective Goldstone descriptions in each phase and low-momentum response functions; soluble lattice versions of our models; the consequences of the dipole symmetry for the Hilbert space; subtleties associated with UV/IR mixing, and the quantization of dipole charges on a lattice; and solutions to the large $N$ Dyson equations in asymptotic limits. We refer the interested and intrepid reader there.

There are three lessons from our analysis that we highlight here, which we expect will be relevant for models with conserved dipole moment more generally. (1) The quartic interactions involving spatial derivatives in these models are crucial and in general cannot be treated perturbatively. They generate a momentum-dependent self-energy, which tames loop integrals. (2) The dipole symmetry is spontaneously broken. At high temperature, so that the ordinary global symmetry is unbroken, we find the low-energy Goldstone description of the continuum theory in the Supplemental Material [21]. This effective theory was proposed in [34], and is Gaussian in the deep IR. The low-temperature phase also has a Gaussian Goldstone description in the infrared, as proposed in [18]. These effective theories are perhaps best suited to describe systems with approximate dipole symmetry upon adding small breaking terms. (3) The coarse-grained model is weakly sensitive to the details of an underlying lattice. We already encountered one such sensitivity. In finite volume, the dipole symmetry breaking implies the existence of a UV-sensitive ground state degeneracy. It arises through the volume of the zero modes associated with dipole breaking. That volume diverges in the continuum theory, but with a lattice regulator goes as the number of lattice sites. As we discuss in the Supplemental Material [21], the lack of decoupling of the lattice can be studied in the Goldstone effective descriptions. We emphasize that we were able to study the large $N$ solution without difficulty in the continuum limit, and near the continuum limit.

We conclude with a brief list of future prospects.

In this work we have identified the large $N$ solution of these models, including the large $N$ Green's function. It should be possible to compute the large $N$ four-point function, whose connected part comes from a sum over bubbles. From this one would be able to directly identify the low-energy Goldstone description, compute hydrodynamic response functions, find the free energy to $O(N^0)$, and more.

It has been argued in [14] that the lowest Landau level may be thought of as a theory of fracton order with conserved dipole number, and conserved quadrupole trace. There are large $N$ models with this symmetry. A simple, but trivial example, is to consider a model with conserved dipole moment but vanishing trace of the dipole current, $J^i_i = 0$. In model 1 this can be achieved by setting $\mathrm{Im}(\lambda) = 0$, and in model 2 by a scaling limit with $\lambda_S \to 0$, $\mathrm{Im}(\gamma) = 0$, and $\lambda_S \mathrm{Re}(\gamma)$ fixed. So there are nontrivial large $N$ models with this symmetry pattern.

Relatedly, we may consider large $N$ models with subsystem symmetry. We will report on that topic in the future [35]. See the Supplemental Material [21] for further discussion on a variety of topics.

We would like to thank P. Glorioso, A. Gromov, A. Karch, E. Lake, and S. H. Shao for enlightening

discussions. K. J. is supported in part by an NSERC Discovery Grant, and A. R. is supported by the U.S. Department of Energy under Grant No. DE-SC0022021 and a grant from the Simons Foundation (Grant No. 651678, AK).

*kristanj@uvic.ca
†araz@utexas.edu

[1] C. Chamon, Phys. Rev. Lett. **94**, 040402 (2005).
[2] S. Bravyi, B. Leemhuis, and B. M. Terhal, Ann. Phys. (Asmterdam) **326**, 839 (2011).
[3] J. Haah, Phys. Rev. A **83**, 042330 (2011).
[4] S. Vijay, J. Haah, and L. Fu, Phys. Rev. B **92**, 235136 (2015).
[5] R. M. Nandkishore and M. Hermele, Annu. Rev. Condens. Matter Phys. **10**, 295 (2019).
[6] A. Gromov, Phys. Rev. X **9**, 031035 (2019).
[7] E. Guardado-Sanchez, A. Morningstar, B. M. Spar, P. T. Brown, D. A. Huse, and W. S. Bakr, Phys. Rev. X **10**, 011042 (2020).
[8] J. Sous and M. Pretko, Phys. Rev. B **102**, 214437 (2020).
[9] J. Sous and M. Pretko, Materials **5**, 81 (2020).
[10] M. Pretko and L. Radzihovsky, Phys. Rev. Lett. **120**, 195301 (2018).
[11] A. Gromov, Phys. Rev. Lett. **122**, 076403 (2019).
[12] D. X. Nguyen, A. Gromov, and S. Moroz, SciPost Phys. **9**, 076 (2020).
[13] D. Doshi and A. Gromov, arXiv:2005.03015.
[14] Y.-H. Du, U. Mehta, D. X. Nguyen, and D. T. Son, SciPost Phys. **12**, 050 (2022).
[15] N. Seiberg and S.-H. Shao, SciPost Phys. **10**, 027 (2021).
[16] N. Seiberg and S.-H. Shao, SciPost Phys. **9**, 046 (2020).
[17] S. Vijay, J. Haah, and L. Fu, Phys. Rev. B **94**, 235157 (2016).
[18] M. Pretko, Phys. Rev. B **98**, 115134 (2018).
[19] S. Giombi, S. Minwalla, S. Prakash, S. P. Trivedi, S. R. Wadia, and X. Yin, Eur. Phys. J. C **72**, 2112 (2012).
[20] V. Rosenhaus, J. Phys. A **52**, 323001 (2019).
[21] See Supplemental Material at http://link.aps.org/supplemental/10.1103/PhysRevLett.132.071603 for a number of useful results that go beyond the main text. These include more details about the collective field formulation of our models; lattice versions thereof; details about the representation theory of dipole symmetry on the lattice; and more.
[22] A. Jain and K. Jensen, SciPost Phys. **12**, 142 (2022).
[23] O. Aharony, S. M. Chester, and E. Y. Urbach, J. High Energy Phys. 03 (2021) 208.
[24] L. Dolan and R. Jackiw, Phys. Rev. D **9**, 3320 (1974).
[25] G. Leibbrandt, Rev. Mod. Phys. **47**, 849 (1975).
[26] A. Jain, K. Jensen, R. Liu, and E. Mefford, J. High Energy Phys. 09 (2023) 184.
[27] J. Distler, A. Karch, and A. Raz, J. High Energy Phys. 03 (2022) 016.
[28] E. Witten, Nucl. Phys. **B145**, 110 (1978).
[29] L. Bidussi, J. Hartong, E. Have, J. Musaeus, and S. Prohazka, SciPost Phys. **12**, 205 (2022).
[30] N. Banerjee, J. Bhattacharya, S. Bhattacharyya, S. Jain, S. Minwalla, and T. Sharma, J. High Energy Phys. 09 (2012) 046.
[31] K. Jensen, M. Kaminski, P. Kovtun, R. Meyer, A. Ritz, and A. Yarom, Phys. Rev. Lett. **109**, 101601 (2012).
[32] S. Bhattacharyya, S. Jain, S. Minwalla, and T. Sharma, J. High Energy Phys. 01 (2013) 040.
[33] P. Glorioso, J. Guo, J. F. Rodriguez-Nieva, and A. Lucas, Nat. Phys. **18**, 912 (2022).
[34] E. Lake, M. Hermele, and T. Senthil, Phys. Rev. B **106**, 064511 (2022).
[35] K. Jensen and A. Raz (to be published).